

An improved reversibly dimerizing mutant of the FK506-binding protein FKBP

Juan J. Barrero[#], Effrosyni Papanikou[#], Jason C. Casler, Kasey J. Day, and Benjamin S. Glick

Department of Molecular Genetics and Cell Biology, University of Chicago, Chicago, IL, USA

ABSTRACT

FK506-binding protein (FKBP) is a monomer that binds to FK506, rapamycin, and related ligands. The F36M substitution, in which Phe36 in the ligand-binding pocket is changed to Met, leads to formation of antiparallel FKBP dimers, which can be dissociated into monomers by ligand binding. This FKBP(M) mutant has been employed in the mammalian secretory pathway to generate aggregates that can be dissolved by ligand addition to create cargo waves. However, when testing this approach in yeast, we found that dissolution of FKBP(M) aggregates was inefficient. An improved reversibly dimerizing FKBP formed aggregates that dissolved more readily. This FKBP(L,V) mutant carries the F36L mutation, which increases the affinity of ligand binding, and the I90V mutation, which accelerates ligand-induced dissociation of the dimers. The FKBP(L,V) mutant expands the utility of reversibly dimerizing FKBP.

ARTICLE HISTORY

Received 14 June 2016
Accepted 14 June 2016

KEY WORDS

dimerization; F36M; FKBP;
FK506-binding protein;
regulatable secretory cargo

Introduction

Human FKBP, also known as FKBP12, is a monomeric 12-kDa *cis/trans* peptidyl-prolyl isomerase and a member of a family of proteins that bind the immunosuppressive drugs FK506 and rapamycin.¹² The FKBP-FK506 complex associates with the phosphatase calcineurin, whereas the FKBP-rapamycin complex associates with the FKBP-rapamycin binding (FRB) domain of the kinase mTOR. As a research tool, the FKBP-rapamycin-FRB interaction has been widely used for ligand-inducible heterodimerization of fusion proteins.⁹ The cytotoxicity of rapamycin can be avoided by using synthetic ligands that bind to wild-type or mutant forms of FKBP.

When Phe36 in the ligand-binding pocket of FKBP was changed to Met to create the FKBP(M) mutant, a novel property emerged.³³ The altered ligand-binding interface self-associated so that FKBP(M) formed an antiparallel homodimer, and in the presence of ligand, dimerization was blocked. Expression in mammalian cells of enhanced GFP (EGFP) fused to 4 tandem copies of FKBP(M) resulted in formation of fluorescent aggregates, presumably due to a heterogeneous set of cross-associations between the EGFP-FKBP(M)_{x4} molecules. Those aggregates could be dissolved by adding ligand.

Reversible aggregation of FKBP(M) has been exploited to create cargo waves in the mammalian secretory pathway.³⁰ When EGFP-FKBP(M)_{x4} was targeted to the lumen of the endoplasmic reticulum (ER), it formed aggregates that were too large to exit the ER. Addition of ligand dissolved the aggregates to yield a soluble fluorescent secretory cargo that was incorporated into ER-derived vesicles and transported to the Golgi.

Variations on this method have been used to test models for protein traffic through the Golgi stack.^{20,31,40}

We are interested in using reversible aggregation to create cargo waves in the secretory pathway of the yeast *Saccharomyces cerevisiae*, which is a popular experimental organism for studying membrane traffic.^{18,28} The specific goal is to test whether secretory cargoes remain in a Golgi cisterna while resident Golgi proteins arrive and depart during cisternal maturation.²⁴ This prediction about the behavior of secretory cargoes is crucial for validating the cisternal maturation model.¹⁵ However, no good method is yet available for tracking the movement of fluorescent cargoes through the yeast secretory pathway. We observed that when fluorescent proteins were targeted to the yeast ER, GFP variants exited the ER slowly,¹⁰ but the highly soluble tetrameric DsRed variant E2-Crimson³⁷ exited the ER much faster (E. Papanikou, unpublished observations). E2-Crimson was therefore deemed a good starting point for engineering a fluorescent secretory cargo. Fusion of a single copy of FKBP(M) to tetrameric E2-Crimson was predicted to generate fluorescent aggregates that could be dissolved by adding ligand (Fig. 1).

For initial characterization, we fused FKBP(M) to E2-Crimson and expressed this construct in the yeast cytosol. Fluorescent aggregates formed and could be dissolved by adding ligand. However, dissolution of the aggregates was relatively slow and required high ligand concentrations. To improve this system, we engineered an alternative dimerizing FKBP mutant that permits faster dissolution of aggregates using lower concentrations of ligand.

CONTACT Benjamin S. Glick  bsglick@uchicago.edu  Molecular Genetics & Cell Biology, University of Chicago, 920 East 58th St., Chicago, IL 60637, USA.

[#]These authors contributed equally.

 Supplemental data for this article can be accessed on the [publisher's website](#).

© 2016 Juan J. Barrero, Effrosyni Papanikou, Jason C. Casler, Kasey J. Day, and Benjamin S. Glick. Published with license by Taylor & Francis.

This is an Open Access article distributed under the terms of the Creative Commons Attribution-Non-Commercial License (<http://creativecommons.org/licenses/by-nc/3.0/>), which permits unrestricted non-commercial use, distribution, and reproduction in any medium, provided the original work is properly cited. The moral rights of the named author(s) have been asserted.

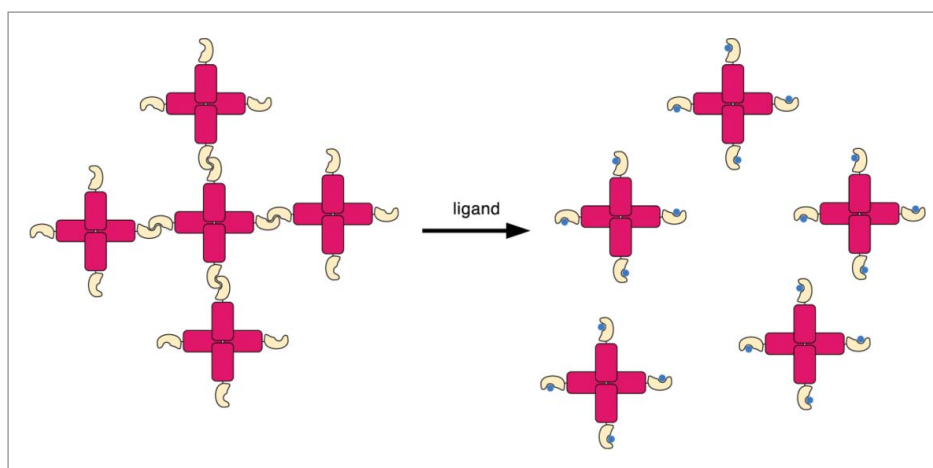


Figure 1. Strategy for generating fluorescent aggregates using dimerizing FKBP. Tetrameric E2-Crimson (red) is fused to a dimerizing FKBP mutant (gold) to generate cross-linked aggregates. Addition of ligand (blue) disrupts FKBP dimerization, thereby yielding soluble tetramers.

Results and discussion

Generation of fluorescent aggregates in the yeast cytosol

It was previously shown that expression in mammalian cells of EGFP fused to 4 tandem copies of FKBP(M) resulted in formation of fluorescent aggregates.³³ To replicate this effect in yeast, we expressed EGFP-FKBP(M)x4 from an integrating vector using the strong constitutive *TPII* promoter. Many of the cells showed one or 2 fluorescent aggregates (Fig. 2A).

EGFP itself has a weak tendency to dimerize, and this property can dramatically affect the localization of certain fusion

proteins.^{22,36,42} We therefore made an alternative yeast expression construct in which EGFP was replaced with mEGFP, which contains the monomerizing A206K mutation.⁴² Yeast cells expressing mEGFP-FKBP(M)x4 showed a diffuse cytosolic fluorescence with few if any aggregates (Fig. 2B). We infer that aggregate formation with EGFP-FKBP(M)x4 likely involves EGFP dimerization as well as FKBP(M) dimerization.

A conceptually simpler way to generate fluorescent aggregates is to fuse a single copy of FKBP(M) to a tetrameric fluorescent protein (see Fig. 1). When FKBP(M) was fused to the C-terminus of E2-Crimson and expressed in yeast, many of the cells showed one or two fluorescent aggregates of varying size (Fig. 3, top panels). By contrast, when FKBP(M) was replaced with wild-type FKBP, none of the cells had fluorescent aggregates (data not shown). Thus, the E2-Crimson-FKBP(M) construct was deemed promising for the generation of reversible aggregates in yeast cells.

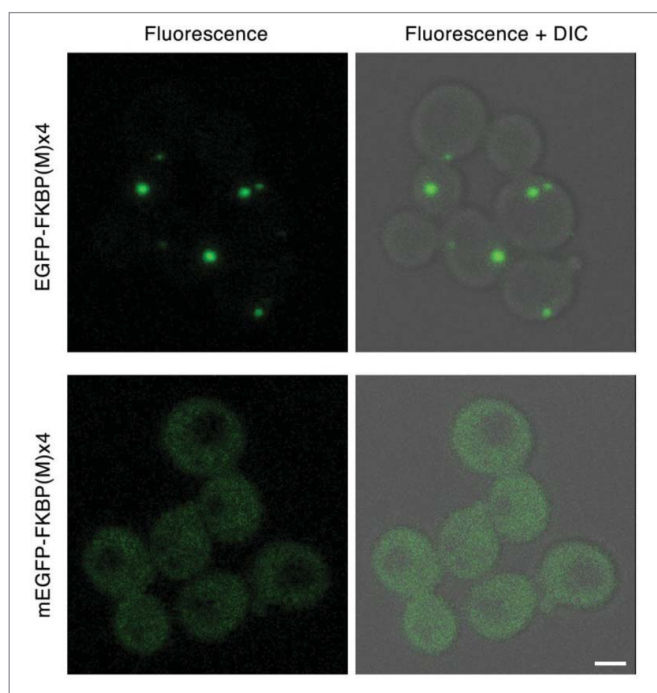


Figure 2. Influence of the fluorescent protein tag on the formation of aggregates containing 4 tandem copies of FKBP(M). Yeast cells were transformed with integrating vectors to express either EGFP-FKBP(M)x4 or mEGFP-FKBP(M)x4. Green fluorescence and differential interference contrast (DIC) images of logarithmically growing cells were captured by confocal microscopy, using the same parameters for both strains. Representative fluorescence and merged images are shown. To enhance weaker signals, the gamma value of the fluorescence images was adjusted to 2.0 using Adobe Photoshop. Scale bar, 2 μ m.

Dissolution of aggregates in a drug-sensitive yeast strain

In an effort to dissolve the E2Crimson-FKBP(M) aggregates, we used a commercially available synthetic ligand of FKBP called SLF.¹⁷ However, when wild-type yeast cells expressing E2-Crimson-FKBP(M) were incubated with 250 μ M SLF for up to 2 h, no significant dissolution of the aggregates was seen (Fig. 3, top panels).

We reasoned that the cells might be removing SLF with the aid of ABC-type pleiotropic drug resistance (PDR) transporter proteins.³² One of the major drug transporters in *S. cerevisiae* is Pdr5. In a *pdr5 Δ mutant expressing E2-Crimson-FKBP(M), treatment for 15 min with SLF led to substantial dissolution of the aggregates, with many cells showing a uniform weak cytosolic fluorescence and others showing cytosolic fluorescence plus very small aggregates (Fig. 3, middle panels). But after 1 h the cytosolic fluorescence was no longer visible, and the cells contained multiple small aggregates. Evidently, the cells adapted over time^{34,38} by increasing their capacity to export SLF using transporters other than Pdr5.*

Expression of Pdr5 and many other PDR proteins in *S. cerevisiae* is controlled by the Pdr1 and Pdr3 pair of transcription factors.³² To achieve a broad and persistent suppression of drug

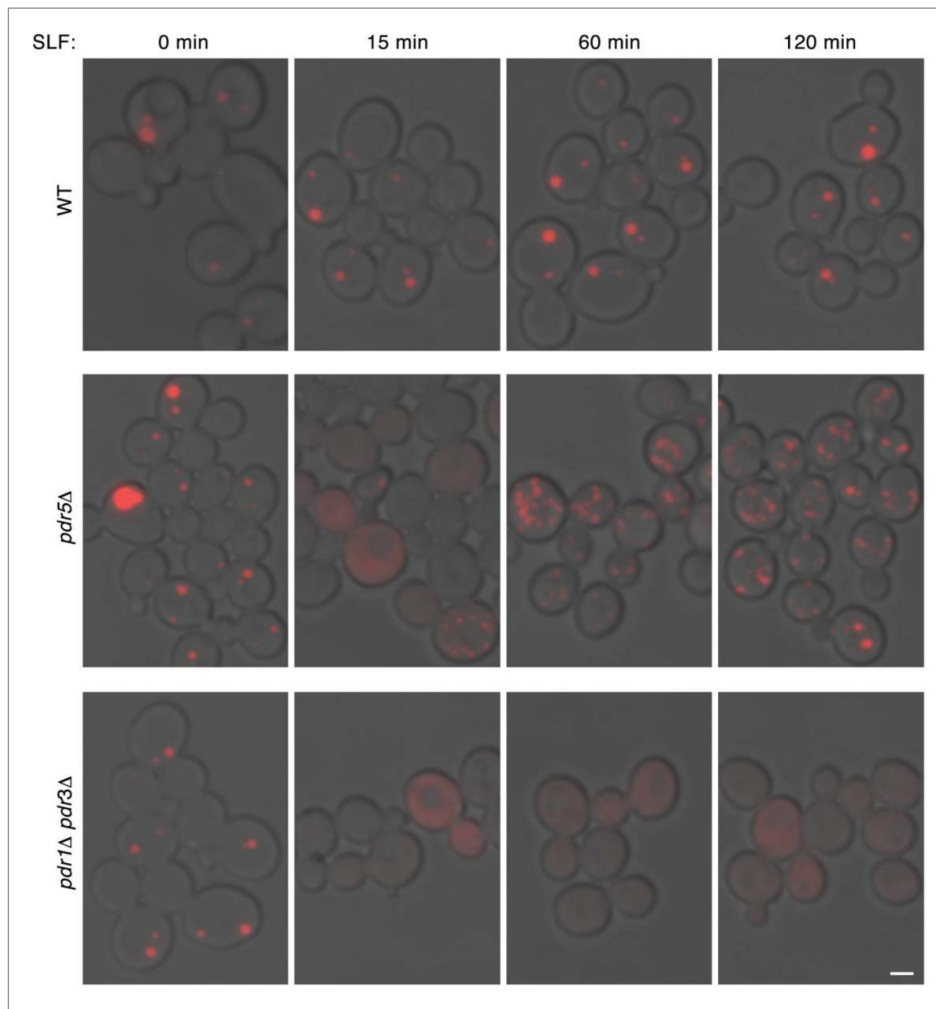


Figure 3. Enhanced aggregate dissolution in drug-sensitive yeast strains. An integrating vector encoding E2-Crimson-FKBP(M) was transformed into isogenic wild-type and *pdr5Δ* and *pdr1Δ pdr3Δ* strains. Logarithmically growing cultures were treated with 250 μ M SLF for 0 to 120 min as indicated, and were imaged by confocal microscopy to capture red fluorescence and DIC images, using the same parameters in all cases. Representative merged images are shown. Scale bar, 2 μ m.

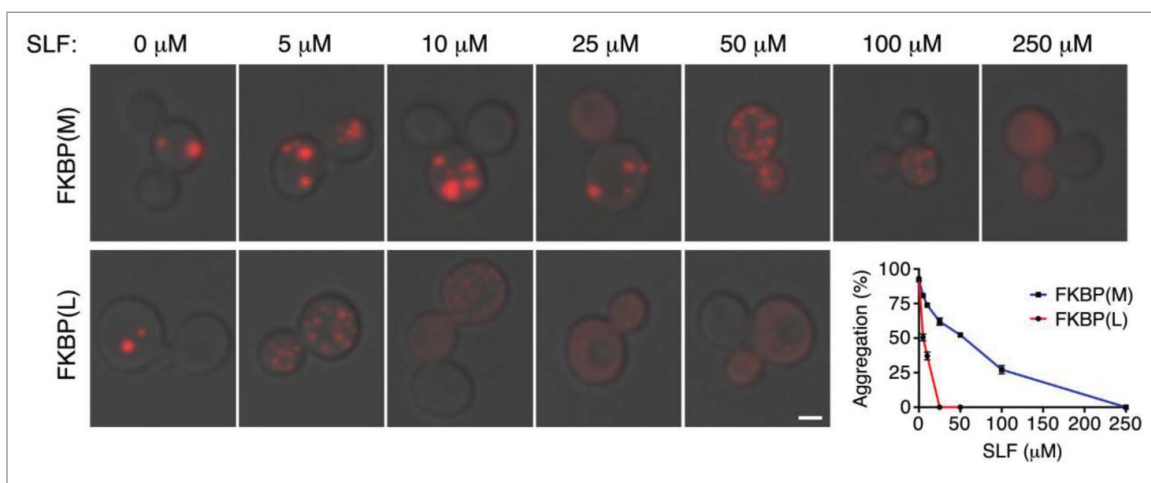


Figure 4. Aggregate dissolution at lower ligand concentrations with the F36L mutation. Integrating vectors encoding E2-Crimson-FKBP(M) or E2-Crimson-FKBP(L) were transformed into a *pdr1Δ pdr3Δ* strain. Logarithmically growing cultures were treated with the indicated concentrations of SLF for 30 min, and were imaged by confocal microscopy to capture red fluorescence and DIC images, using the same parameters in all cases. For each strain and condition, approximately 30 – 100 cells were examined, and the percentage of the fluorescence signal that was punctate was quantified as described in Materials and Methods. Representative merged images are shown together with quantitation of the image data. Scale bar, 2 μ m. Error bars represent s.e.m.

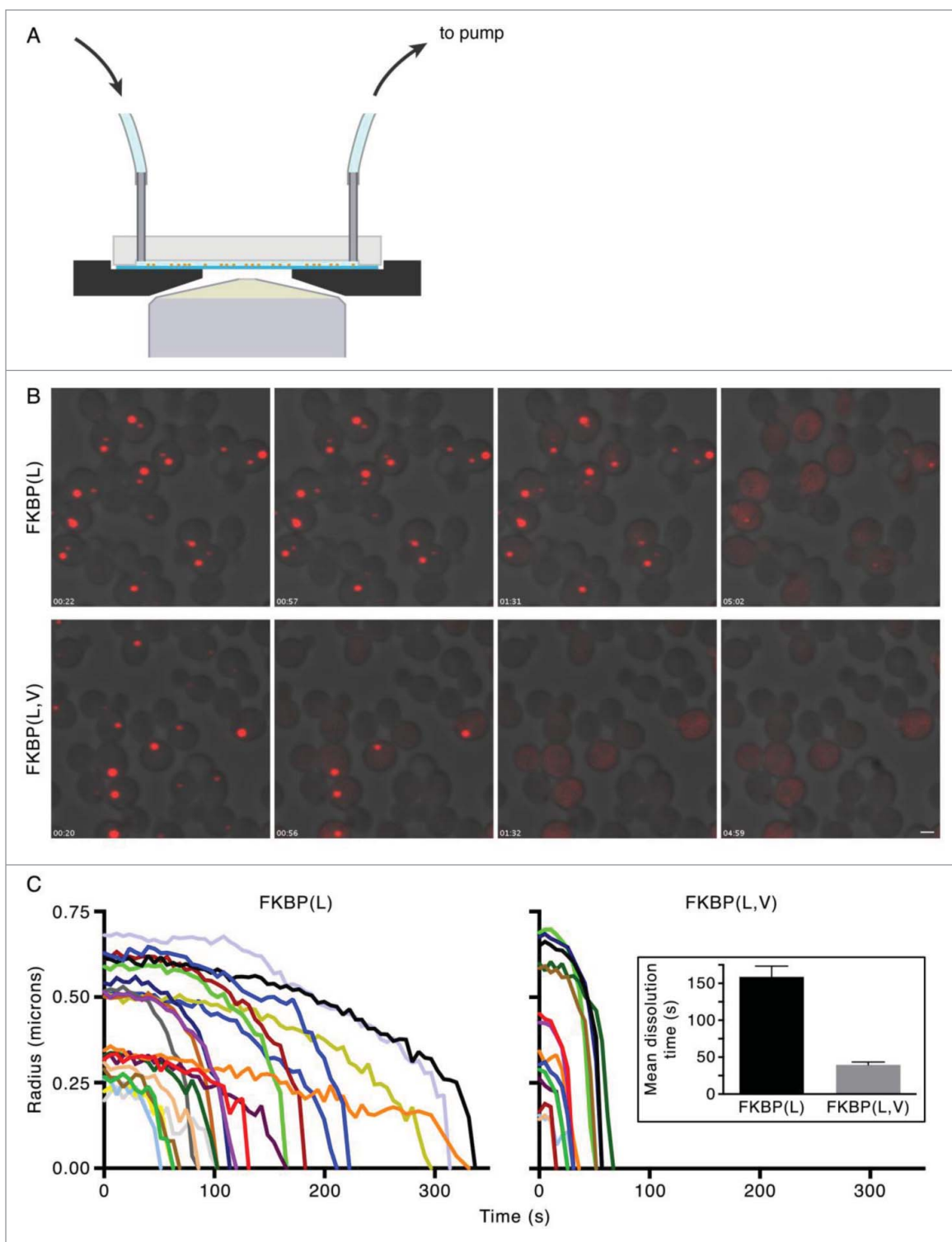


Figure 5. Faster aggregate dissolution with the I90V mutation. (A) Diagram of a cross-section through the center of the flow chamber. Media enters and exits the chamber through Tygon tubing attached to stainless steel tubes embedded in a slab of hard PMMA plastic. Those tubes connect to a groove in the plastic. The PMMA slab is placed on a concanavalin A-coated coverslip to which yeast cells have been attached. This assembly sits in a well in a metal piece on a microscope stage. To hold the assembly in place, an additional clear plastic slab, not shown in the diagram, is placed on top and attached with screws to the metal piece. A tapered opening in the metal piece allows an oil objective to be positioned close to the bottom of the coverslip. Medium is pulled through the flow chamber using a negative pressure pump. Hydrophobic compounds such as SLF flow directly past the cells. (B) Selected frames from Videos 1 and 2, which show SLF-induced dissolution of E2-Crimson-FKBP(L) aggregates and E2-Crimson-FKBP(L,V) aggregates, respectively. SLF reached the cells approximately 20 s after the beginning of a movie. Scale bar, 2 μm . (C) Quantitation of aggregate dissolution from Videos 1 and 2. The radius of each fluorescent aggregate was measured at each time point, beginning at the time point when SLF was estimated to reach the cells. The inset shows the mean time needed for complete dissolution of aggregates. For this quantitation, a total of 43 E2-Crimson-FKBP(L) aggregates and 36 E2-Crimson-FKBP(L,V) aggregates were examined from 3 movies for each construct, and the times needed for complete dissolution of the aggregates were recorded. Error bars represent s.e.m. The mean dissolution times were 159 ± 15 s for E2-Crimson-FKBP(L) and 40 ± 4 s for E2-Crimson-FKBP(L,V).

export, we disrupted both the *PDR1* and *PDR3* genes. In a *pdv1Δ pdv3Δ* double mutant expressing E2-Crimson-FKBP(M), addition of SLF dissolved the aggregates to generate a uniform cytosolic fluorescence that persisted for at least 2 h (Fig. 3, bottom panels, and data not shown). The *pdv1Δ pdv3Δ* strain was therefore chosen as the starting point for further analysis.

Enhancement of the ligand effect with the F36L mutation

To dissolve E2-Crimson-FKBP(M) aggregates, we used SLF at 250 μ M because lower concentrations were less effective. A *pdv1Δ pdv3Δ* strain showed no growth defect in medium containing 250 μ M SLF (data not shown), but the use of such high drug concentrations is expensive and raises concerns about nonspecific effects on the cells. These issues could be addressed by identifying a dimerizing FKBP variant with stronger ligand binding.

The F36M mutation reduces ligand binding affinities approximately 10-fold,³³ whereas the F36L mutation has only a minimal effect on ligand binding.⁸ A possible ability of the F36L mutation to promote dimerization has not been reported. We therefore tested whether dimerization occurred with an F36L mutant of FKBP, here termed FKBP(L). Indeed, E2-Crimson-FKBP(L) formed cytosolic aggregates similar to those seen with E2-Crimson-FKBP(M) (Fig. 4).

The prediction was that E2-Crimson-FKBP(L) aggregates would dissolve at lower SLF concentrations than E2-Crimson-FKBP(M) aggregates. For this experiment, *pdv1Δ pdv3Δ* cells expressing the aggregating constructs were incubated with varying concentrations of SLF for 30 min. Confocal image stacks were then acquired, and the ratio of punctate to total fluorescence was quantified. Representative images are shown in Figure 4 together with quantitation of the image data. Maximal dissolution of E2-Crimson-FKBP(M) aggregates required 250 μ M SLF, whereas maximal dissolution of E2-Crimson-FKBP(L) aggregates required only 25 μ M SLF. Thus, the F36L mutation is apparently preferable to F36M for the purpose of ligand-reversible dimerization.

Acceleration of aggregate shrinkage with the I90V mutation

After addition of SLF, aggregates generated with E2-Crimson-FKBP(M) or E2-Crimson-FKBP(L) required up to 5 min or more for complete dissolution. Because a similar time scale is seen for cargo transport through the yeast secretory pathway²⁴ and our ultimate goal is to produce a nearly synchronous cargo wave, faster dissolution of the aggregates would be useful.

Ligand-induced disruption of the FKBP dimer presumably occurs when the dimer spontaneously dissociates to enable ligand binding. Therefore, a mutation that increases the dissociation rate of the dimer would be expected to accelerate ligand-induced shrinkage of FKBP aggregates. To identify such a mutation, we examined the crystal structure of the FKBP(M) dimer.³³ Residue Ile-90 in the dimerization interface has a hydrophobic interaction with its counterpart in the other subunit. The corresponding residue is Val in many closely related FKBP proteins,¹¹ suggesting that the less hydrophobic Val should be tolerated at position 90. We introduced the I90V mutation into FKBP(L) to generate FKBP(L,V).

To visualize the shrinkage of aggregates containing E2-Crimson fused to either FKBP(L) or FKBP(L,V), we sought to perform live-cell imaging after addition of SLF. Flow chambers have been described for introducing drugs during live-cell imaging of yeast,^{4,21} but those systems were constructed using the polymer polydimethylsiloxane (PDMS), which binds hydrophobic drugs such as SLF.⁴³ We therefore modified and simplified a commercially available yeast live-cell imaging system⁴ to avoid the use of PDMS. As shown in Figure 5A, yeast cells attached to a coverslip with concanavalin A are overlaid with a slab of the hard plastic poly(methyl methacrylate) (PMMA). A channel in the PMMA creates a flow chamber, which is connected to metal tubes that are connected in turn to plastic tubing. Liquid is pulled through the chamber by a nonelectric pressure-driven pump.²⁵ With this device, we can flow SLF-containing medium over the cells while performing 4D confocal microscopy.

This flow chamber was used to track the shrinkage of cytosolic E2-Crimson-FKBP(L) and E2-Crimson-FKBP(L,V) aggregates after addition of 25 μ M SLF. The stacks of confocal images for the individual time points were projected, and the projections were assembled into movies. Figure 5B shows frames from 2 representative movies (Videos 1 and 2). The aggregates varied considerably in size, and accordingly, they took variable amounts of time to dissolve. On average, shrinkage of aggregates was substantially faster with E2-Crimson-FKBP(L,V) than with E2-Crimson-FKBP(L). In Figure 5C, the radii of the aggregates from the 2 representative movies are plotted as a function of time. The inset to Figure 5C shows that with E2-Crimson-FKBP(L,V) the mean time for complete dissolution of an aggregate was only 40 sec, approximately 4 times less than with E2-Crimson-FKBP(L). Thus, the I90V mutation substantially accelerates shrinkage of aggregates.

Conclusions

Reversible aggregates can be generated in the secretory pathway not only with dimerizing FKBP, but also with tools such as the plant photoreceptor protein UVR8, which forms photolabile homodimers.⁵ Another way to create a secretory cargo wave is the “retention using selective hooks” (RUSH) system, which employs biotin to release a streptavidin-binding peptide-modified reporter protein from a streptavidin-modified ER-localized hook protein.³ Each of these methods is likely to have advantages and disadvantages for particular applications. Because dimerizing FKBP has proven to be useful and flexible, we are seeking to adapt it for generating reversible aggregates in the yeast secretory pathway.

As the first step in this project, we used rational mutagenesis to improve the properties of dimerizing FKBP. The widely used FKBP(M) mutant has the F36M mutation, which promotes dimerization but also reduces ligand binding affinities.³³ By contrast, the F36L mutation was reported to have only a minimal effect on ligand binding affinities,⁸ and we found that the FKBP(L) mutant dimerizes. Aggregates generated with FKBP(L) dissolve at about 10-fold lower ligand concentrations than aggregates generated with FKBP(M).

Another opportunity for improvement concerned the speed of ligand-induced disruption of the dimer. The dimer dissociates spontaneously at some rate, enabling ligand to bind and to occlude the dimerization interface. Based on this reasoning, we

examined the crystal structure of the FKBP(M) dimer, and noted that hydrophobic interactions involving Ile-90 probably contribute to dimerization.³³ We therefore replaced Ile-90 with Val, which is structurally similar but less hydrophobic. The I90V mutation is expected to accelerate spontaneous dissociation of the dimer. Consistent with this prediction, aggregates generated with the FKBP(L,V) mutant, which has both the F36L and I90V mutations, shrink about 4-fold faster after ligand addition than aggregates generated with FKBP(L).

Our characterization of the dimerizing FKBP mutants employed the synthetic FKBP ligand SLF to dissolve fluorescent aggregates in the yeast cytosol, and this approach allowed us to overcome 2 technical hurdles. The first hurdle was that SLF can be exported from yeast cells by drug transporters. Drug resistance is commonly observed in yeast, and is often addressed by deleting genes that encode drug transporters such as Pdr5.³² However, in a *pdr5*Δ strain, SLF has only a transient effect. A likely explanation is that SLF stimulates the synthesis of other drug transporters by means of the transcription factors Pdr1 and Pdr3.^{32,34,38} Consistent with this interpretation, in a *pdr1*Δ *pdr3*Δ mutant, SLF persistently dissolves the aggregates. These results emphasize the value of the *pdr1*Δ *pdr3*Δ combination for obtaining long-lasting sensitivity to a range of drugs.⁶ The second hurdle was that SLF is readily absorbed by the plastic PDMS, which is typically used to make flow chambers for live cell imaging. Anecdotally, similar problems are observed with a variety of commonly used hydrophobic drugs, including compounds that disrupt the cytoskeleton (D. Kovar, personal communication). We devised a simple PDMS-free flow chamber that enables SLF to be introduced during live cell imaging. This approach should be useful for diverse experiments in which drugs are applied to yeast or other cell types.

The goal is to apply these advances toward generation of a secretory cargo wave in yeast, but additional technical issues will need to be addressed. For example, translocation of soluble proteins into the yeast ER typically follows a posttranslational pathway,^{1,26} and because E2-Crimson-FKBP(L,V) can fold and oligomerize in the cytosol, this fusion protein is unlikely to cross the ER membrane posttranslationally. A solution is to use the Ost1 signal sequence, which promotes cotranslational translocation^{29,41} and efficiently targets proteins to the ER lumen before they have a chance to fold.¹⁰ Our initial tests indicate that a pre-Ost1-E2-Crimson-FKBP(L,V) construct forms aggregates in the ER lumen, and that the aggregates can be dissolved by SLF (unpublished data). However, export of the solubilized fusion protein from the ER is slow, presumably because export occurs by bulk flow.³⁹ This limitation can potentially be overcome by appending an ER export signal such as the pro region of pre-pro- α -factor.^{10,27} Finally, to visualize the fluorescent secretory cargo together with early and late Golgi markers, we will need to extend our protocol for whole-cell 2-color confocal imaging^{7,24} to 3 colors. We are working to overcome these challenges in order to visualize secretory cargo traffic in living yeast.

Materials and methods

Strains, plasmids, and reagents

The parental haploid *S. cerevisiae* strain was JK9-3da (*leu2*-3,112 *ura3*-52 *rme1* *trp1* *his4*).¹⁹ Yeast cells were grown in

minimal glucose dropout medium (SD)³⁵ or nonfluorescent minimal medium (NSD)² prepared using nutrient mixtures from Sunrise Science Products (San Diego, CA). The *PDR5* and *PDR1* genes were disrupted by PCR-based gene deletion using a kanamycin resistance cassette,²³ and the *PDR3* gene was disrupted in a similar manner using a nourseothricin resistance cassette.¹⁶

DNA constructs were designed with the aid of SnapGene software (GSL Biotech, Chicago, IL), and the Supplemental Materials includes a folder of 5 annotated plasmid map/sequence files that can be opened with SnapGene Viewer (www.snapgene.com/products/snapgene_viewer). Expression with the integrating vector YIplac204¹³ was driven by the strong constitutive *TPI1* promoter and the *CYC1* terminator.²⁴ Plasmids were modified by standard methods including primer-directed mutagenesis and Gibson assembly, and critical regions were verified by sequencing. Integrating vectors were linearized and then transformed into yeast cells using lithium acetate¹⁴ for integration at the *TRP1* locus. Single-copy integrations were confirmed by PCR using primers 5'GTGTACTTTGCGATTATGACGCCAGATG G3' and 5'AGTCAACCCCCTGCGATGTATATTTTCCTG3'.

A 100 mM solution of SLF in ethanol was obtained from Cayman Chemical (Ann Arbor, MI). This drug was diluted in NSD to the desired concentration.

Construction of the flow chamber

A Warner Instruments model YC-1 yeast cell flow chamber, which was based on a published design,⁴ was modified as follows. The device was supplied with a PDMS flow chamber containing 1.27-mm outer diameter stainless steel perfusion port tubes that terminated in a 100- μ m deep groove in the chamber. Those tubes were removed, and were inserted into a custom fabricated PMMA slab of the same size with a similar groove. The YC-1 chamber immobilizes yeast cells by gently compressing them between a cellulose membrane and a PDMS-coated coverslip. Instead, we omitted the cellulose membrane, and immobilized the cells on a 24×50 mm high precision No. 1.5 coverslip (Marienfeld, Lauda-Königshofen, Germany) that had been coated with concanavalin A as described below under “Fluorescence microscopy.” The assembly was sealed with a clear top plate that was screwed into place. With this configuration, the medium flowed directly over the cells and never encountered PDMS.

Medium was flowed into the chamber through 1/32" Tygon tubing connected to the stainless steel perfusion port tubes. To minimize leakage, the flow was driven using negative pressure. We employed an inexpensive nonelectric pressure-driven pump,²⁵ with a tank volume created using 4 140-cc syringes (Healthcare Supply Pros, Austin, TX) that were clamped with the plungers in an extended position using 1.5 × 4 inch EZ White Snap Clamps (Amazon.com). Pressure was created using a 60-cc syringe that was clamped with the plunger in an extended position using a 0.75 × 4 inch EZ White Snap Clamp. This setup allowed medium to be flowed over the cells for 10–15 minutes at a rate of approximately 1 mL/min. Presumably, similar results could be obtained using a more conventional electric syringe pump to generate negative pressure.

Fluorescence microscopy

Static images of cells were captured as Z-stacks using a Zeiss LSM 880 confocal microscope equipped with a 1.4-NA 63x oil objective. The Z-stacks were average projected using ImageJ (<https://imagej.nih.gov/ij/>).

For 4D live-cell imaging,⁷ a 5-mL yeast culture was grown overnight in NSD in a baffled flask, and was diluted to an OD₆₀₀ of 0.5–0.7 in fresh NSD medium. A 24 × 50 mm coverslip was coated with freshly dissolved 2 mg/mL concanavalin A (Sigma-Aldrich, St. Louis, MO; product number C2010) for 10 min, then washed with water and allowed to dry. A 250- μ L aliquot of the culture was overlaid on the coverslip, and cells were allowed to adhere for 10 min, followed by several rounds of gentle washing with NSD. The coverslip was placed in the flow chamber and sealed while ensuring that the cells remained immersed in NSD the entire time. NSD was pushed through the flow chamber with a syringe to remove any bubbles, and then the Tygon tubing was clamped. The flow chamber was placed on the stage of a Leica SP5 inverted confocal microscope equipped with a 1.4NA 63x oil objective. One end of the Tygon tubing was connected to the negative pressure pump while the other end was placed in a culture tube with SLF-containing medium. To initiate flow of medium, the clamp was removed. Z-stacks were captured at intervals of 5–6 sec.

Individual images were resized, cropped, and processed to adjust brightness and contrast using Adobe Photoshop. To quantify the fraction of a fluorescent construct that was aggregated at a given SLF concentration, a custom ImageJ plugin was used as described in the Supplemental Materials. 4D data sets were converted to videos using ImageJ.⁷ To quantify the radius of a fluorescent aggregate at a given time point in a video, a maximum intensity projection of the confocal image stack was processed with ImageJ by calibrating the image in microns, setting a threshold that excluded cytoplasmic signal, and using the Analyze Particles tool to measure the area of the aggregate. The radius was then calculated by dividing the square root of the area by π . To determine the time needed for dissolution of a fluorescent aggregate, the aggregate was tracked using maximum intensity projections until it was no longer visible.

Abbreviations

DIC	differential interference contrast
EGFP	enhanced GFP
FKBP	FK506-binding protein
NSD	nonfluorescent synthetic glucose medium
PDMS	polydimethylsiloxane
PMMA	poly(methyl methacrylate); SLF, synthetic ligand of FKBP.

Disclosure of potential conflicts of interest

No potential conflicts of interest were disclosed.

Funding

This work was supported by NIH grant R01 GM104010. Development of the flow chamber was supported by funding through the Biological

Systems Science Division, Office of Biological and Environmental Research, Office of Science, US. Dept. of Energy, under Contract DE-AC02-06CH11357. The negative pressure pump was constructed with the assistance of Cari Launier at the Microenvironmental Control Foundry at the University of Illinois, Chicago, a facility sponsored by the Chicago Biomedical Consortium with support from the Searle Funds at The Chicago Community Trust. JCC and KJD were supported by NIH training grant T32 GM007183. Fluorescence microscopy was performed with the assistance of Vytautas Bindokas at the Integrated Microscopy Core Facility, which received support from the NIH-funded Cancer Center Support Grant P30 CA014599. Fernando Valbuena helped to optimize the PCR-based method for confirming single-copy integrations.

References

- [1] Ast T, Cohen G, Schuldiner M. A network of cytosolic factors targets SRP-independent proteins to the endoplasmic reticulum. *Cell* 2013; 152:1134-45; PMID:23452858; <http://dx.doi.org/10.1016/j.cell.2013.02.003>
- [2] Bevis BJ, Hammond AT, Reinke CA, Glick BS. *De novo* formation of transitional ER sites and Golgi structures in *Pichia pastoris*. *Nat Cell Biol* 2002; 4:750-6; PMID:12360285; <http://dx.doi.org/10.1038/ncb852>
- [3] Boncompain G, Divoux S, Gareil N, de Forges H, Lescure A, Latreche L, Mercanti V, Jollivet F, Raposo G, Perez F. Synchronization of secretory protein traffic in populations of cells. *Nat Methods* 2012; 9:493-8; PMID:22406856; <http://dx.doi.org/10.1038/nmeth.1928>
- [4] Charvin G, Oikonomou C, Cross F. Long-term imaging in microfluidic devices. *Methods Mol Biol* 2010; 591:229-42; PMID:19957134; http://dx.doi.org/10.1007/978-1-60761-404-3_14
- [5] Chen D, Gibson ES, Kennedy MJ. A light-triggered protein secretion system. *J Cell Biol* 2013; 201:631-40; PMID:23671313; <http://dx.doi.org/10.1083/jcb.201210119>
- [6] Coorey NVC, Matthews JH, Bellows DS, Atkinson PH. Pleiotropic drug-resistance attenuated genomic library improves elucidation of drug mechanisms. *Mol Biosyst* 2015; 11:3129-36; PMID:26381459; <http://dx.doi.org/10.1039/C5MB00406C>
- [7] Day KJ, Papanikou E, Glick BS. 4D confocal imaging of yeast organelles. *Methods Mol. Biol.* 2016, in press
- [8] DeCenzo MT, Park ST, Jarrett BP, Aldape RA, Futer O, Murcko MA, Livingston DJ. FK506-binding protein mutational analysis: defining the active-site residue contributions to catalysis and the stability of ligand complexes. *Protein Eng* 1996; 9:173-80; PMID:9005438; <http://dx.doi.org/10.1093/protein/9.2.173>
- [9] Fegan A, White B, Carlson JC, Wagner CR. Chemically controlled protein assembly: techniques and applications. *Chem Rev* 2010; 110:3315-36; PMID:20353181; <http://dx.doi.org/10.1021/cr8002888>
- [10] Fitzgerald I, Glick BS. Secretion of a foreign protein from budding yeasts is enhanced by cotranslational translocation and by suppression of vacuolar targeting. *Microb Cell Fact* 2014; 13:125; PMID:25164324; <http://dx.doi.org/10.1186/s12934-014-0125-0>
- [11] Galat A. Functional drift of sequence attributes in the FK506-binding proteins (FKBPs). *J Chem Inf Model* 2008; 48:1118-30; PMID:18412331; <http://dx.doi.org/10.1021/ci700429n>
- [12] Galat A. Functional diversity and pharmacological profiles of the FKBPs and their complexes with small natural ligands. *Cell Mol Life Sci* 2013; 70:3243-75; PMID:23224428; <http://dx.doi.org/10.1007/s00018-012-1206-z>
- [13] Gietz RD, Sugino A. New yeast-*Escherichia coli* shuttle vectors constructed with in vitro mutagenized yeast genes lacking six-base pair restriction sites. *Gene* 1988; 74:527-34; PMID:3073106; [http://dx.doi.org/10.1016/0378-1119\(88\)90185-0](http://dx.doi.org/10.1016/0378-1119(88)90185-0)
- [14] Gietz RD, Woods RA. Transformation of yeast by lithium acetate/single-stranded carrier DNA/polyethylene glycol method. *Methods Enzymol* 2002; 350:87-96; PMID:12073338; [http://dx.doi.org/10.1016/S0076-6879\(02\)50957-5](http://dx.doi.org/10.1016/S0076-6879(02)50957-5)
- [15] Glick BS, Luini A. Models for Golgi traffic: a critical assessment. *Cold Spring Harb Perspect Biol* 2011; 3:a005215; PMID:21875986; <http://dx.doi.org/10.1101/cshperspect.a005215>

- [16] Goldstein AL, McCusker JH. Three new dominant drug resistance cassettes for gene disruption in *Saccharomyces cerevisiae*. *Yeast* 1999; 15:1541-53; PMID:10514571; [http://dx.doi.org/10.1002/\(SICI\)1097-0061\(199910\)15:14%3c1541::AID-YEA476%3e3.0.CO;2-K](http://dx.doi.org/10.1002/(SICI)1097-0061(199910)15:14%3c1541::AID-YEA476%3e3.0.CO;2-K)
- [17] Holt DA, Luengo JI, Yamashita DS, Oh HJ, Konialian AL, Yen HK, Rozamus LW, Brandt M, Bossard MJ, Levy MA, et al. Design, synthesis, and kinetic evaluation of high-affinity FKBP ligands and the X-ray crystal structures of their complexes with FKBP12. *J Am Chem Soc* 1993; 115:9925-38; <http://dx.doi.org/10.1021/ja00075a008>
- [18] Kaiser CA, Gimeno RE, Shaywitz DA. Protein secretion, membrane biogenesis, and endocytosis. In: *The Molecular and Cellular Biology of the Yeast Saccharomyces*, vol. 3, eds. JR Pringle, JR Broach, and EW Jones. Cold Spring Harbor, NY: Cold Spring Harbor Laboratory Press, 1997, 91-227.
- [19] Kunz J, Schneider U, Deuter-Reinhard M, Movva NR, Hall MN. Target of rapamycin in yeast, TOR2, is an essential phosphatidylinositol kinase homolog required for G1 progression. *Cell* 1993; 73:585-96; PMID:8387896; [http://dx.doi.org/10.1016/0092-8674\(93\)90144-F](http://dx.doi.org/10.1016/0092-8674(93)90144-F)
- [20] Lavieu G, Zheng H, Rothman JE. Stapled Golgi cisternae remain in place as cargo passes through the stack. *eLife* 2013; 2:e00558; PMID:23755362; <http://dx.doi.org/10.7554/eLife.00558>
- [21] Lee PJ, Helman NC, Lim WA, Hung PJ. A microfluidic system for dynamic yeast cell imaging. *BioTechniques* 2008; 44:91-5; PMID:18254385; <http://dx.doi.org/10.2144/000112673>
- [22] Lisenbee CS, Karnik SK, Trelease RN. Overexpression and mislocalization of a tail-anchored GFP redefines the identity of peroxisomal ER. *Traffic* 2003; 4:491-501; PMID:12795694; <http://dx.doi.org/10.1034/j.1600-0854.2003.00107.x>
- [23] Longtine MS, McKenzie A, 3rd, Demarini DJ, Shah NG, Wach A, Brachet A, Philippsen P, Pringle JR. Additional modules for versatile and economical PCR-based gene deletion and modification in *Saccharomyces cerevisiae*. *Yeast* 1998; 14:953-61; PMID:9717241; [http://dx.doi.org/10.1002/\(SICI\)1097-0061\(199807\)14:10%3c953::AID-YEA293%3e3.0.CO;2-U](http://dx.doi.org/10.1002/(SICI)1097-0061(199807)14:10%3c953::AID-YEA293%3e3.0.CO;2-U)
- [24] Losev E, Reinke CA, Jellen J, Strongin DE, Bevis BJ, Glick BS. Golgi maturation visualized in living yeast. *Nature* 2006; 22:1002-6; PMID:16699524; <http://dx.doi.org/10.1038/nature04717>
- [25] Moscovici M, Chien WY, Abdelgawad M, Sun Y. Electrical power free, low dead volume, pressure-driven pumping for microfluidic applications. *Biomicrofluidics* 2010; 4:46501; PMID:21057609; <http://dx.doi.org/10.1063/1.3499939>
- [26] Ng DT, Brown JD, Walter P. Signal sequences specify the targeting route to the endoplasmic reticulum membrane. *J Cell Biol* 1996; 134:269-78; PMID:8707814; <http://dx.doi.org/10.1083/jcb.134.2.269>
- [27] Otte S, Barlowe C. Sorting signals can direct receptor-mediated export of soluble proteins into COPII vesicles. *Nat Cell Biol* 2004; 6:1189-94; PMID:15516922; <http://dx.doi.org/10.1038/ncb1195>
- [28] Papanikou E, Glick BS. The yeast Golgi apparatus: insights and mysteries. *FEBS Lett* 2009; 583:3746-51; PMID:19879270; <http://dx.doi.org/10.1016/j.febslet.2009.10.072>
- [29] Pechmann S, Chartron JW, Frydman J. Local slowdown of translation by nonoptimal codons promotes nascent-chain recognition by SRP *in vivo*. *Nat Struct Mol Biol* 2014; 21:1100-05; PMID:25420103; <http://dx.doi.org/10.1038/nsmb.2919>
- [30] Rivera VM, Wang X, Wardwell S, Courage NL, Volchuk A, Keenan T, Holt DA, Gilman M, Orci L, Cerasoli FJ, et al. Regulation of protein secretion through controlled aggregation in the endoplasmic reticulum. *Science* 2000; 287:826-30; PMID:10657290; <http://dx.doi.org/10.1126/science.287.5454.826>
- [31] Rizzo R, Parashuraman S, Mirabelli P, Puri C, Lucocq J, Luini A. The dynamics of engineered resident proteins in the mammalian Golgi complex relies on cisternal maturation. *J Cell Biol* 2013; 201:1027-36; PMID:23775191; <http://dx.doi.org/10.1083/jcb.201211147>
- [32] Rogers B, Decottignies A, Kolaczowski M, Carvajal E, Balzi E, Goffeau A. The pleiotropic drug ABC transporters from *Saccharomyces cerevisiae*. *J Mol Microbiol Biotechnol* 2001; 3:207-14; PMID:11321575
- [33] Rollins CT, Rivera VM, Woolfson DN, Keenan T, Hatada M, Adams SE, Andrade LJ, Yaeger D, van Schravendijk MR, Holt DA, et al. A ligand-reversible dimerization system for controlling protein-protein interactions. *Proc Natl Acad Sci USA* 2000; 97:7096-101; PMID:10852943; <http://dx.doi.org/10.1073/pnas.100101997>
- [34] Schüller C, Mammun YM, Wolfger H, Rockwell N, Thorner J, Kuchler K. Membrane-active compounds activate the transcription factors Pdr1 and Pdr3 connecting pleiotropic drug resistance and membrane lipid homeostasis in *Saccharomyces cerevisiae*. *Mol Biol Cell* 2007; 18:4932-44; PMID:17881724; <http://dx.doi.org/10.1091/mbc.E07-06-0610>
- [35] Sherman F. Getting started with yeast. *Methods Enzymol* 1991; 194:3-21; PMID:2005794; [http://dx.doi.org/10.1016/0076-6879\(91\)94004-V](http://dx.doi.org/10.1016/0076-6879(91)94004-V)
- [36] Snapp EL, Hegde RS, Francolini M, Lombardo F, Colombo S, Pedrazzini E, Borgese N, Lippincott-Schwartz J. Formation of stacked ER cisternae by low affinity protein interactions. *J Cell Biol* 2003; 163:257-69; PMID:14581454; <http://dx.doi.org/10.1083/jcb.200306020>
- [37] Strack RL, Hein B, Bhattacharyya D, Hell SW, Keenan RJ, Glick BS. A rapidly maturing far-red derivative of DsRed-Express2 for whole-cell labeling. *Biochemistry* 2009; 48:8279-81; PMID:19658435; <http://dx.doi.org/10.1021/bi900870u>
- [38] Thakur JK, Arthanari H, Yang F, Pan SJ, Fan X, Breger J, Frueh DP, Gulshan K, Li DK, Mylonakis E, et al. A nuclear receptor-like pathway regulating multidrug resistance in fungi. *Nature* 2008; 452:604-9; PMID:18385733; <http://dx.doi.org/10.1038/nature06836>
- [39] Thor F, Gautschi M, Geiger R, Helenius A. Bulk flow revisited: transport of a soluble protein in the secretory pathway. *Traffic* 2009; 10:1819-30; PMID:19843282; <http://dx.doi.org/10.1111/j.1600-0854.2009.00989.x>
- [40] Volchuk A, Amherdt M, Ravazzola M, Brugger B, Rivera VM, Clackson T, Perrelet A, Söllner TH, Rothman JE, Orci L. Megavesicles implicated in the rapid transport of intracisternal aggregates across the Golgi stack. *Cell* 2000; 102:335-48; PMID:10975524; [http://dx.doi.org/10.1016/S0092-8674\(00\)00039-8](http://dx.doi.org/10.1016/S0092-8674(00)00039-8)
- [41] Willer M, Forte GM, Stirling CJ. Sec61p is required for ERAD-L: genetic dissection of the translocation and ERAD-L functions of Sec61p using novel derivatives of CPY. *J Biol Chem* 2008; 283:33883-8; PMID:18819915; <http://dx.doi.org/10.1074/jbc.M803054200>
- [42] Zacharias DA, Violin JD, Newton AC, Tsien RY. Partitioning of lipid-modified monomeric GFPs into membrane microdomains of live cells. *Science* 2002; 296:913-6; PMID:11988576; <http://dx.doi.org/10.1126/science.1068539>
- [43] Zhou J, Khodakov DA, Ellis AV, Voelcker NH. Surface modification for PDMS-based microfluidic devices. *Electrophoresis* 2012; 33:89-104; PMID:22128067; <http://dx.doi.org/10.1002/elps.201100482>